Journal of Medical Devices Technology

jmeditec.utm.my

Original Research

A Study of The Effect of Model Geometry and Body Mass Index on The Elastohydrodynamic Lubrication Performance of Metal-on-Metal Hip Joints

Hasan Basri[1*], Tri Satya Ramadhoni[2], Akbar Teguh Prakoso[1], Muhammad Imam Ammarullah[3,4], J. Jamari[5,6]

[1] *Department of Mechanical Engineering, Faculty of Engineering, Universitas Sriwijaya, South Sumatra 30662, Indonesia.*
[2] *Department of Mechanical Engineering, Faculty of Engineering, Universitas Tamansiswa, West Sumatra 25171, Indonesia*
[3] *Department of Mechanical Engineering, Faculty of Engineering, Universitas Pasundan, Bandung 40153, West Java, Indonesia*
[4] *Biomechanics and Biomedics Engineering Research Centre, Universitas Pasundan, Bandung 40153, West Java, Indonesia*
[5] *Undip Biomechanics Engineering & Research Centre (UBM-ERC), Universitas Diponegoro, Semarang 50275, Central Java, Indonesia*
[6] *Department of Mechanical Engineering, Faculty of Engineering, Universitas Diponegoro, Semarang 50275, Central Java, Indonesia*

ARTICLE INFO

Article History:
Received 24 December 2021
Accepted 29 June 2022
Available online 1 Sept 2022

Keywords:
Artificial hip joint,
Ball-on-plane,
Body mass index,
Elastohydrodynamic.

ABSTRACT

This study aims to provide benefits on the manufacturing side in considering design parameters for optimization of total hip arthroplasty based on body mass index (BMI) categories. The femoral and cup geometries in Total Hip Arthoplasty (THA) are modeled in a simple ball-on-plane form to analyze the pressure and thickness of the lubricant film in the elastohydrodynamic lubrication of artificial hip joints with vertical loads and parameters based on body mass index using the finite element method. The factor of being overweight is one of the causes of increasing the maximum load during activities. This study applies a maximum load based on BMI which is divided into two categories, namely normal and high BMI to obtain the distribution of contact pressure and fluid pressure on the bearing surfaces that are in contact with each other so that the thickness of the lubricating film formed can be determined. Validation of contact pressure and film thickness was carried out. The femoral head sizes applied were 24mm and 28mm with a radial clearance of 15µm, 30µm and 100µm using CoCrMo metal material. From the simulation the load at high BMI shows an increase by a large enough difference reaching 16.89MPa at contact pressure, 19.88MPa at fluid pressure and 0.004µm at the thickness of the lubricant film compared to normal BMI. This simple modeling provides the benefit of analyzing the effect of body mass index on tribological THA performance and can help reduce the growth rate of THA implantation failure revision surgery.

INTRODUCTION

Total Hip Arthoplasty (THA) is a surgical procedure that consists of the physical replacement of an unhealthy natural human synovial joint with an artificial hip joint. This artificial connection must guarantee several aspects, namely biocompatibility, fixation, mobility, load capacity, stability, minimal friction and wear in a tribological system. From a tribological point of view, in order to reduce implant failure and the rate of revision numbers, researchers are still studying the phenomenon of lubrication and looking for the optimal configuration of the combination bearing material combination parameters. This study used metal to metal material and the radius of the femoral head was 12 mm and 14 mm. The data was obtained from the Mohammad Hoesin Hospital in Palembang. The radius size and the type of material selected are the most frequently used data. During normal running conditions metal against metal has a low wear rate. Even though it has a low wear rate, the direct contact that occurs in metal to metal can release metal ions in the bloodstream which can spread throughout the body and cause a local inflammatory reaction in the tissues which can eventually lead to osteolysis. High contact pressures can result in high wear of metal-to-metal bearings. This is because wear and contact pressure are directly proportional to the possibility of causing the initial THA failure for metallosis and aseptic loosening. This is in accordance with previous

* Hasan Basri
Department of Mechanical Engineering, Faculty of Engineering, Universitas Sriwijaya, South Sumatra 30662, Indonesia.

research (Karachalios et al., 2018). which said that metal particles from the wear that occurs in metal bearings against metal can cause aseptic loosening and metallosis. In non-obese patients, the initial revision of metallosis reached 18.3% and aseptic loosening reached 56.5%. In obese patients, revision metallosis at the beginning reached 56.5% and aseptic loosening reached 71.4%. Minimizing the wear that occurs on metal to metal is essential to reduce the risk of adverse toxic side effects. So far, previous research has only aimed at optimization of THA implants, including optimization topology, geometric dimensions and addition of dimples (Basri et al., 2019; Ramadhoni et al., 2020; Basri et al., 2019) with the aim of increasing hydrodynamic pressure and increasing the thickness of the lubrication film and material modification to minimize wear. Even though there are internal factors that can have an effect on poor results, namely body mass index towards obesity which results in an increase in complications of failure after THA implantation surgery. The increasing rate of THA revision surgery in obese THA implantation failure includes cases of aseptic loosening, metallosis, fracture, and instability (Jeschke et al., 2018; Goodnough et al. 2018). The relationship of obesity to the specific causes of failure (mechanical failure) in THA implants has not been studied in detail. Therefore, the aim of this study was to obtain the effect of body mass index (BMI) on implant failure in terms of tribological engineering in the form of contact pressure distribution, fluid pressure, and lubricant film thickness based on the influence of radial clearance distance and femoral head size at hip bone joints. made of metal to metal.

MATERIALS AND METHOD

Dimensions and Materials

Three-dimensional modeling of the artificial hip joint was created in a ball-on-plane form using Comsol Multiphysic 5.4 software. Symmetrical ball-on-plane modeling is simplified into quarter parts. The use of the model refers to research (Mattei et al., 2010) that the semi-elastic half-space theory, the hipbone joint can be simplified into an equivalent ball-on-plane model. The fixation system consisting of cement and bone is neglected without losing accuracy. Numerical simulations were performed using Comsol Multiphysic 5.4 software to analyze the variations in the radial clearance distance and the size of the femoral head diameter based on normal and high body mass index. The material used is the CoCrMo material with a diameter variation of 24 mm and 28 mm and the results of patient data observation at the Mohammad Hoesin General Hospital in Palembang for the period November 2018-June 2019. The following is the observation data that shows the diameter of the femoral head as shown in Table 1.

Table 1 The size of the femoral head implant diameter is often used at the Mohammad Hoesin General Hospital in Palembang for the period November 2018-May 2019.

Month	The size of the implant diameter femoral head		Amount (unit)
	24 mm	28 mm	
November 2018	2	3	5
December 2018	1	3	4
January 2019	5	4	9
February 2019	3	1	4
March 2019	5	1	6
April 2019	4	2	6
May 2019	3	1	4
June 2019	0	1	1
Total	23	16	39

Based on Table 1, the patients have two sizes of femoral head, namely 24 mm and 28 mm with a diameter of 24 mm was used more than the size of 28 mm.

To develop the assumed semi-infinite plane, the geometric dimensions of the plane that are symmetrical are considered to be 40 times the length and 20 times the width of the contact radius (a). The dimensions of the length and width of the plane geometry refer to previous studies (Noori-Dokht et al., 2017). The dimensions of the femoral head diameter used in this study were 24 mm and 28 mm and the metal material was *CoCrMo* (E=210 GPa, v=0.3, ρ=9150 kg/m^3) (Askari et al., 2015; Aherwar et al., 2015). This data is taken based on data from patients with artificial hip joints that are often used at the Mohammad Hoesin General Hospital in Palembang from November to 2018 to June 2019. The radial clearance used are 15 µm, 30 µm and 100 µm which is based on previous research data (Tsikandylakis et al. 2018). The symmetrical three-dimensional ball-on-plane model is shown in Figure 1.

Meshing of geometry

The three-dimensional model of the ball-on-plane finite element method was created using Comsol Multiphysic 5.4 software. Meshing uses triangular elements on the boundary of the lubricant film which focuses on the density of the element at the centre point and the tetrahedral element in the solid domain as shown in Figure 2.

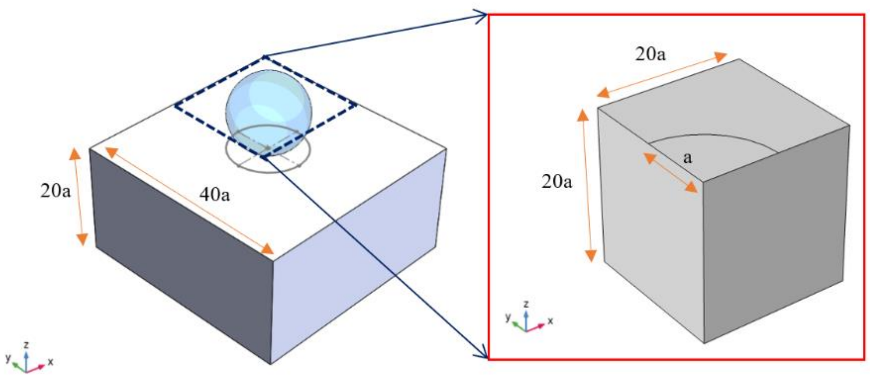

Fig. 1 (a) Symmetrical three-dimensional ball-on-plane model, (b) Simplify the ball-on-plane into quarters.

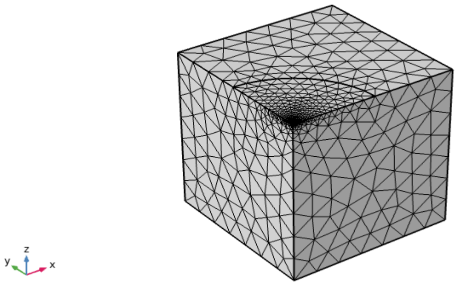

Fig. 2 Meshing on a ball-on-plane model.

Solid domain boundary conditions

Material in the solid domain is assumed to be linear elastic. Vertical direction of loading with concentrated point contact on the solid domain. The boundary conditions are symmetrical on a quarter ball-on-plane which are seen from the z axis (x, y) and y axis (x, z) as shown in Figure 3.

Fluid domain boundary condition

Lubricants are assumed to be Newtonian, incompressible and no slip wall conditions. The viscosity for the lubricant is assumed to be 0.01 Pa s. The viscosity for the lubricant is assumed to be 0.01 Pa.s (Mattei et al., 2010). Reynolds equation which has been simplified (Ramachandran, 2014) is applied to obtain fluid pressure and lubricant film thickness in a symmetrical geometric model as follows:

$$\frac{1}{r}\frac{\partial}{\partial r}\left(rh^3\frac{\partial pf}{\partial r}\right)=12\eta\frac{\partial h}{\partial t} \tag{1}$$

The calculation is limited to the range $0<r<R$. Equation (1) is applied with the boundary conditions $\frac{\partial pf}{\partial r}=0$ at $r=0$ and $pf=0$ at the lubricant boundary or when $r=R'$. Where R' is the effective radius of the radius of the femoral head and acetabular cup, pf is the distribution of fluid pressure and r is the horizontal radial distance from the center of the boundary of the lubricant circle.

Loading on ball-on-plane geometry for artificial hip joints

The ball-on-plane configuration is determined by the radius of the femoral head and the equivalent acetabular cup which refers to the previous study calculated using equation (2) (Jalali-Vahid et al., 2000). The contact Hertzian theory for elastic stress in the ball-on-plane was developed to determine the radius of contact of the deforming entities on the surface with vertical loads calculated by equation (3, 4 and 5). The fluid domain boundary conditions is shown in Figure 4.

$$a=\sqrt[3]{\frac{3WzR'}{2E'}} \tag{2}$$

$$p\max=\frac{3Wy}{2\pi a^2} \tag{3}$$

$$p(x,y)=p\max\sqrt{1-\frac{x}{a^2}-\frac{y}{a^2}} \tag{4}$$

$$E'=\frac{2}{\frac{1-\vartheta_1^2}{E_1}+\frac{1-\vartheta_2^2}{E_2}} \tag{5}$$

Loading condition in normal running motion

The World Health Organization (WHO) defines body mass index (BMI) into 6 classes, namely the underweight class with an index value of less than (<18.5 kg/m^2), normal weight is at the index value (18.5-24.9 kg/m^2), overweight body has an index value (25.0-29.9 kg/m^2), obesity class 1 with a body mass index value greater than or equal to (30 kg/m^2), obesity class 2 with a body mass index value greater than or equal to (35 kg/m^2) and obesity class 3 with a body mass index value greater than or equal to (40 kg/m^2).. In this study the body mass indexes used are the first category (normal BMI) and the second category (high BMI with class obesity 1), with index values (22.0 kg/m^2) and (31.1 kg/m^2) respectively. The first category has a maximum force value of 2730 N and the second category is 3880 N. In this study, we use a load at a maximum point, namely when the heel is off as shown in Figure 5 and there is no flexion or extension rotational motion so that this study focuses on the load with translational motion.

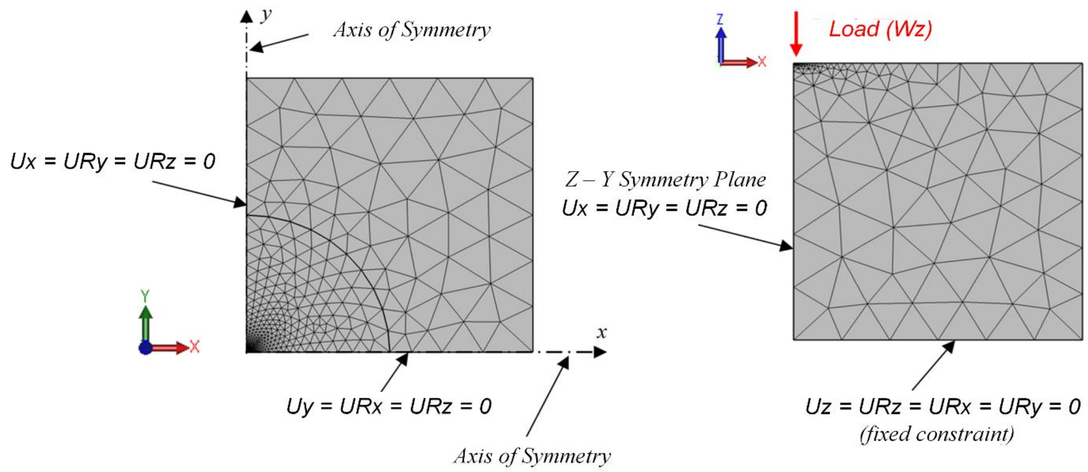

Fig. 3 The boundary conditions of symmetrical on a quarter ball-on-plane (a) the view is from z axis (x, y) and (b) the view is from y axis (x, z).

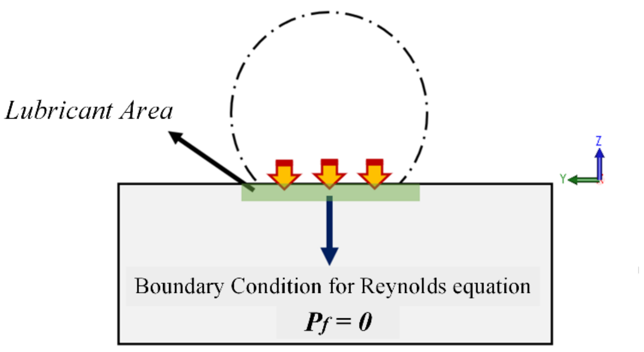

Fig. 4 Fluid domain boundary conditions.

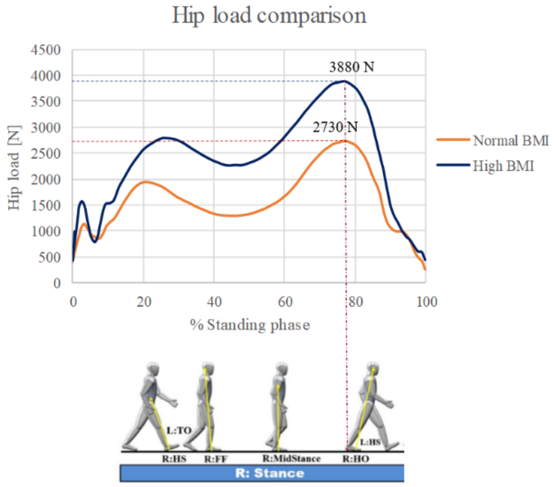

Fig. 5 Comparison of hip load during standing phase at heel off (HO) in walking motion at normal and high body mass index.

RESULT AND DISCUSSION

Convergence studies

Convergence studies have been carried out on the femoral head and acetabular cup bearings based on the simulation results of contact pressure using metal to metal materials and vertical loads of 2500N. Figure 6 shows the convergence mesh results to contact pressure with the selected element size is 1.13 mm where the value of contact pressure obtained has a stable finite element solution accuracy of 50.67 MPa so that the increase in the number of elements can be stopped. The number of elements used reached 38,673 elements and the variation in element sizes was between 0.47 mm and 2.99 mm.

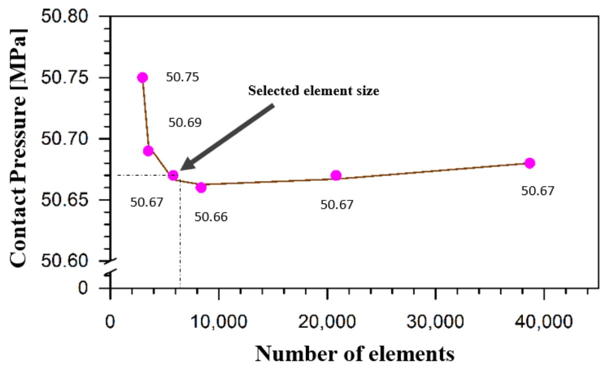

Fig. 6 The result of the mesh converges to contact pressure.

Effect of clearance on contact pressure based on BMI

The numerical approach using the finite element method to obtain the effect of radial clearance on maximum contact pressure based on the category of normal and high body mass index were carried out on two sizes of the radius of the femoral head, namely 12mm and 14mm. Figure 7a and Figure 7b show the effect of clearance on maximum contact pressure based on BMI at 12 mm and 14 mm radius of femoral head, respectively.

Based on Figure 7a that with increasing radial clearance, the contact pressure also increases. The data show an increase from 40.69 MPa to 139.21 MPa at normal BMI and from 45.76 MPa to 156.1 MPa at high BMI. The effect of body mass index on contact pressure on the radial clearance of 15 µm, 30 µm, and 100 µm, respectively show that the difference also increases with increasing radial clearance distance from 5.07 MPa, 7.64 MPa to 16.89 MPa. Based on Figure 7b, the increase in the radial clearance increases the contact pressure. The data show an increase from 32.9 MPa to 113.75 MPa at normal BMI and from 37.15 MPa to 127.56 MPa at high BMI. For the effect of body mass index on contact pressure on the radial clearance distance of 15 µm, 30 µm, and 100 µm, respectively show that the difference also increases with increasing radial clearance distance from 4.25 MPa, 6.33 MPa to 13.81 MPa.

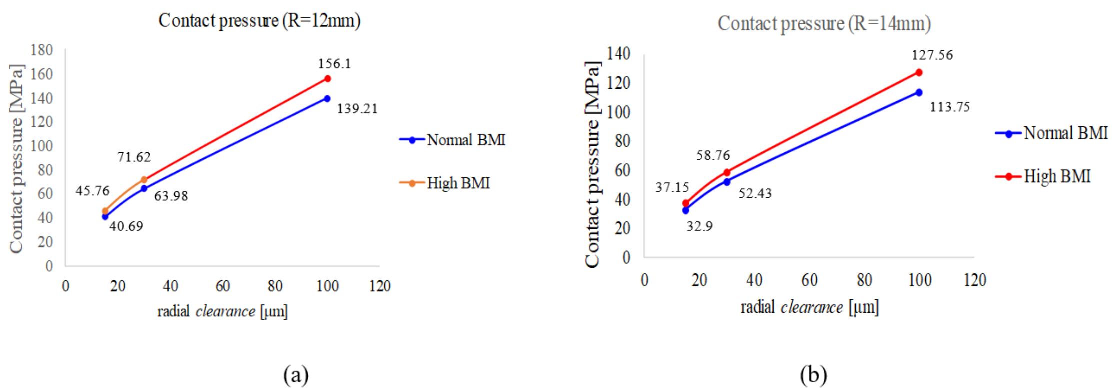

Fig. 7 Comparison of the contact pressure distribution of different femoral head radius with the variation of the radial clearance to normal and high BMI. (a) Radius femoral head 12 mm and (b) Radius femoral head 14 mm.

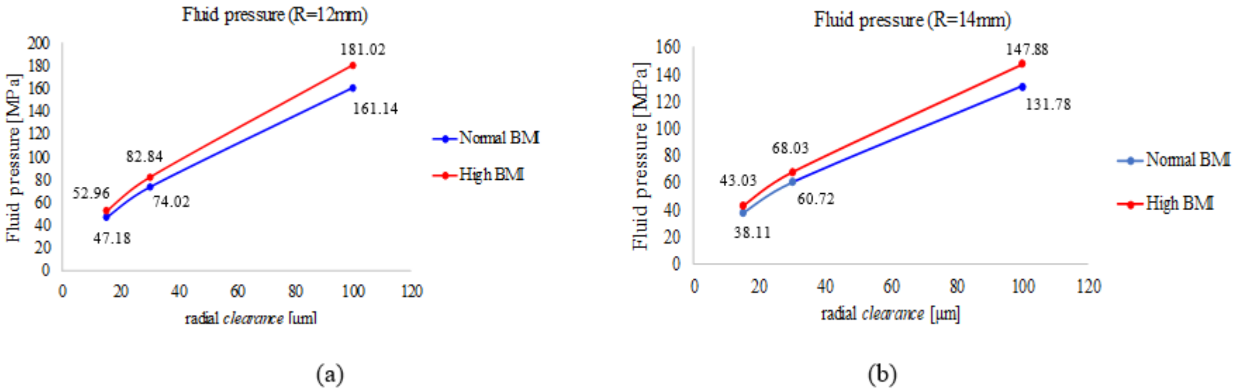

Fig. 8 Comparison of the fluid pressure distribution of different femoral head radius with the variation of the radial clearance to normal and high BMI: (a) Radius femoral head 12 mm and (b) Radius femoral head 14 mm.

Effect of clearance on fluid pressure based on BMI

The numerical approach using the finite element method to obtain the effect of radial clearance on fluid pressure based on the category of normal and high body mass index (BMI) were carried out on two sizes of the radius of the femoral head 12mm and 14mm. Figure 8a and Figure 8b show the effect of clearance on fluid pressure based on BMI at 12 mm and 14 mm radius of femoral head, respectively.

Based on Figure 8a, it shows that with increasing radial clearance, the fluid pressure also increases. The data show an increase from 47.18 MPa to 161.14 MPa at normal BMI and from 52.96 MPa to 181.02 MPa at high BMI. The effect of body mass index on fluid pressure on the radial clearance distance of 15 µm, 30 µm, and 100 µm, respectively, show that the difference also increases with increasing radial clearance distance from 5.78 MPa, 8.82 MPa to 19.88 MPa. Based on Figure 8b, it shows that the increase in the radial clearance increases the fluid pressure. The data show an increase from 38.11 MPa to 131.78 MPa at normal BMI and from 43.03 MPa to 147.88 MPa at high BMI. The effect of body mass index on fluid pressure with the radial clearance distance of 15 µm, 30 µm, and 100 µm, respectively, show that the difference also increases with increasing radial clearance distance from 4.92 MPa, 7.31 MPa to 16.1 MPa.

The effect of clearance on film thickness based on BMI

A numerical approach using the finite element method to obtain the effect of radial clearance on minimum film thickness based on the category of normal and high body mass index (BMI) was carried out on two sizes of radius of the femoral head, namely 12mm and 14mm. Figure 9a and Figure 9b show the effect of clearance on minimum film thickness based on BMI at 12 mm and 14 mm radius of femoral head, respectively.

Based on Figure 9a that with the increasing of radial clearance will derease the thickness of the lubricant film. The data showed a decrease from 0.091 µm to 0.019 µm at normal BMI and from 0.092 µm to 0.018 µm at high BMI. For the effect of body mass index on the thickness of the lubricant film formed on the radial clearance of 15 µm, 30 µm, and 100 µm, each showed a very small difference as the radial clearance distance increased. Based on Figure 9b that with the increasing radial clearance will decrease the minimum film thickness. The data showed a decrease from 0.116 µm to 0.025 µm at normal BMI and from 0.12 µm to 0.025 µm at high BMI. For the effect of body mass index on the thickness of the lubricant film formed on the radial clearance distance of 15 µm, 30 µm, and 100 µm, respectively shows a very small difference as the radial clearance distance increases from 0.004 µm, 0.002 µm to 0 µm or none.

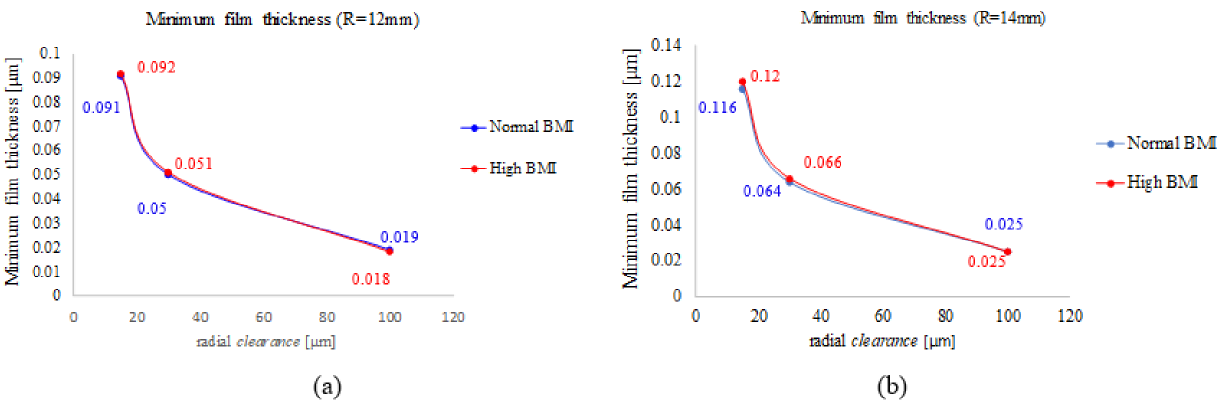

Fig. 9 Comparison of the minimum film thickness of different femoral head radius with the variation of the radial clearance to normal and high BMI: (a) Radius femoral head 12 mm and (b) Radius femoral head 14 mm.

CONCLUSION

Obesity in patients who are dominated by excessive external forces can have an impact on the tribological performance of THA. Base on the results, the contact pressure, fluid pressure and film thickness from normal to high BMI (obesity class 1) were increased almost 12.13%, 10.98% and 0.64%, respectively at radial clearance of 100 μm. Suppose for the patient with BMI above > 40 kg/m^2, the patient should undergo therapy to reduce body weight before planned surgery. It is very important to reduce the revised growth rate due to premature failure of THA as well as to improve the patient's quality of life. The large radial clearance causes an increase in contact pressure and fluid pressure by 110.34 MPa and 128.06 MPa, respectively. The higher the radial clearance size, the smaller the film thickness value. BMI has very little effect on film thickness.

ACKNOWLEDGEMENT

The research publication of this article was funded by DIPA of Public Service Agency of Universitas Sriwijaya 2022. SP DIPA-023.17.2.677515/2022, on Desember 13, 2021. In accordance with the Rector's Decree Number: 0111/UN9.3.1/SK/2022, on April 28, 2022. We gratefully thank the Mechanical Engineering Department, Faculty of Engineering, Universitas Sriwijaya for their strong support of this study, along with the Medical Device and Technology Center (MEDITEC), Institute of Human-Centered and Engineering (iHumEn), Universiti Teknologi Malaysia and the Department of Mechanical Engineering, Faculty of Engineering, Diponegoro University for their encouragement and many fruitful discussions on this research.

REFERENCES

Aherwar, A., Singh, A. K., Patnaik, A. 2016. Current and future biocompatibility aspects of biomaterials for hip prosthesis. AIMS Bioengineering 3, 23-43.

Askari, E., Flores, P., Dabirrahmani, D., Appleyard, R. 2016. A Review of Squeaking in Ceramic Total Hip Prostheses. Tribology International. 93, 239-256.

Basri, H., Syahrom, A., Prakoso, A. T., Wicaksono, D., Amarullah, M. I., Ramadhoni, T. S., Nugraha, R. D. 2019. The Analysis of Dimple Geometry on Artificial Hip Joint to the Performance of Lubrication. Journal of Physics: Conference Series 1198, 1–10.

Basri, H., Syahrom, A., Ramadhoni, T., S., Prakoso, A. T., Ammarullah, M. I., Vincent. 2019. The Analysis of the Dimple Arrangement of the Artificial Hip Joint to the Performance of Lubrication. IOP Conference Series: Materials Science and Engineering 620, 1–10.

Goodnough, L. H., Finlay, A. K., Huddleston, J. I., Goodman, S. B., Maloney, W. J., Amanatullah, D. F. 2018. Obesity is Independently Associated with Early Aseptic Loosening in Primary Total Hip Arthroplasty. Journal of Arthroplasty 33, 882–886.

Jalali-Vahid, D., Jagatia, M., Jin, Z. M., Dowson, D. 2000. Elastohydrodynamic Lubrication Analysis of UHMWPE Hip Joint Replacements. Tribology Series 38, 329-339.

Jeschke, E., Citak, M., Günster, C., Halder, A. M., Heller, Malzahn, K., Jürgen, F. U. Niethard, P. S., Zacher, J., Gehrke, T. 2018. Obesity Increases the Risk of Postoperative Complications and Revision Rates Following Primary Total Hip Arthroplasty: An Analysis of 131,576 Total Hip Arthroplasty Cases. Journal of Arthroplasty 33, 2287-2292.

Karachalios, T., Komnos, G., Koutalos, A. 2018. Total Hip Arthroplasty: Survival and Modes of Failure. EFORT Open Reviews 3, 232–239.

Mattei, L., Ciulli, E., Puccio, F. D., Piccigallo, B. 2010. EHL Modelling of Hard-on-Hard Hip Implants: Comparison of Total and Resurfacing Hip Implants. European Biomechanics 21, 10-22.

Noori-Dokht, H., Niroomand-Oscuii, H., Jalali-Vahid, D., Jin, Z. 2017. Finite Element Analysis of Elastohydrodynamic Lubrication in an Artificial Hip Joint under Squeeze Film Motion Using Fluid-Structure Interaction Method. Proceedings of the Institution of Mechanical Engineers, Part J: Journal of Engineering Tribology 231, 1171–1183.

Ramachandran, P. A. 2014. Advanced Transport Phenomena: Analysis, Modeling, and Computations. Modelling Implant 22, 103-123.

Ramadhoni, T. S., Syahrom, A., Saad, A. P. M., Prakoso, A. T., Wicaksono, D., Basri, H. 2020. The Analysis of Wear on Artificial Hip Joint with Dimple on Femoral Surface. Journal of Physics: Conference Series 1500, 11-22.

Tsikandylakis, G., Mohaddes, M., Cnudde, P., Eskelinen, A., Kärrholm, J., Rolfson, O. 2018. Head Size in Primary Total Hip Arthroplasty. EFORT Open Reviews 3, 225–231.